ELSEVIER

Polymer 43 (2002) 1849–1856

polymer

www.elsevier.com/locate/polymer

Equilibrium solubility of CO_2 in rubbery EVA over a wide pressure range: effects of carbonyl group content and crystallinity

Yeong-Tarng Shieh*, Yen-Gu Lin

Department of Chemical Engineering, National Yunlin University of Science and Technology, 123 University Road, Section 3, Touliu, Yunlin 640, Taiwan, ROC

Received 6 August 2001; received in revised form 25 October 2001; accepted 26 November 2001

Abstract

The equilibrium CO_2 sorption isotherms and isobars for rubbery EVA containing various amounts of vinyl acetate (VA) over a wide pressure range 10–340 atm and 25–52 °C were investigated. The normalized CO_2 sorption concentration (in cm^3 (STP) CO_2/mole VA) isotherms of these polymers as a function of pressure consisted of two distinct regions turning at near P_c. The normalized sorption isotherms in these two distinct regions could be fairly described by two respective power laws: $C = K_a P^{n_a}$ for above P_c and $C = k_b P^{n_b}$ for below P_c. The normalized CO_2 sorption isotherms were found to be about the same for four EVA samples having different VA contents for below P_c, suggesting that the sorption process at below P_c may be mainly driven by the presence of carbonyl groups. At above P_c, the degree of crystallinity of the polymer appeared to be a major factor to affect the sorption process, with the higher the degree of crystallinity, the lower the normalized CO_2 sorption concentration in the polymer. The sorption isobars of the polymer as a function of temperature were governed by the interplay of density, viscosity, and diffusivity of CO_2 depending on the pressure studied.

Keywords: Isotherms; Isobars; Power law

1. Introduction

The carbon dioxide (CO_2) sorption isotherms for glassy polymers, when plotted versus CO_2 pressures, were reported to follow the dual mode sorption model [1–11] in which the total sorption concentration C was expressed by a combination of the Langmuir-type sorption for low pressures and the Henry's law dissolution for high pressures. Koros and Paul [3] reported that the total CO_2 sorption concentration in poly(ethylene terephthalate) (PET) at above T_g over a pressure range 0–20 atm followed the Henry's law model while the dual mode sorption model applied in the glassy state. The CO_2 sorption isotherm for cellulose acetate at pressures up to 45 atm followed also the dual mode sorption model at below T_g of the polymer [11]. In Berens and Huvard's work [7], dual mode CO_2 sorption isotherm (the curvature is concave downward) was shown to be characteristic of the glassy state of a polymer, but the curvature was upward for the rubbery state over a pressure range 0–65 atm. In Kamiya and coworkers' work [8], a different type of CO_2 sorption isotherm for poly(vinyl benzoate) was observed at below T_g. This different type of isotherm was concave downward in the low-pressure region but turned into a straight line with increasing CO_2 pressure (up to 50 atm) that could be extrapolated back to the coordinate origin. In another Kamiya and coworker's work [12], the curvature of CO_2 sorption isotherms for EVA was upward with respect to the pressures axis up to 50 atm and was well described by a simplified Flory–Huggins dissolution model [13] where the Henry's law dissolution concentration C_D was considered as a function of total sorption concentration C as in Eq. (1).

$$C_D = S(C)P = [k_D \exp(\sigma C)]P \quad (1)$$

where $S(C) = [k_D \exp(\sigma C)]$ is a solubility coefficient [9], k_D is the Henry's law parameter, P is pressure, and σ is the constant related to Flory–Huggins interaction parameter χ (i.e. $\sigma = 2(1 + \chi)V/22{,}410$, where V is partial molar volume of the dissolved CO_2) [13]. According to the reports described earlier, neither model was a universal model implying that the nature of polymer and/or the pressure range affect the sorption isotherms.

Glass transition temperature of EVA (poly(ethylene-*co*-vinyl acetate)) in this study is well below 25 °C depending on the copolymer composition. EVA is thus in rubbery state

---

* Corresponding author. Tel.: +886-5-534-2601x4614; fax: +886-5-531-2071.

E-mail address: shiehy@pine.yuntech.edu.tw (Y.-T. Shieh).

0032-3861/02/$ - see front matter
PII: S0032-3861(01)00776-5

above 25 °C. According to Koros and coworkers [3], the CO_2 sorption isotherms for EVA, if measured above 25 °C, should be linear and follow the Henry's law dissolution model over the pressure range 0–20 atm. As reported by Kamiya and coworkers [12], however, the Henry's law without a modification was apparently not able to satisfactorily describe the isotherms of the rubbery EVA over the pressure range 0–50 atm. In addition, CO_2 is not an ideal gas (particularly true at high pressures) and its properties (such as density, viscosity, intermolecular attraction force, and diffusivity) are not linearly proportional to pressures. These CO_2 properties (especially the density) are even considerably varied with pressures near the critical conditions (72.8 atm and 31.1 °C). The CO_2 sorption isotherms for high pressures crossing P_c might, thus, significantly deviate from the Henry's law. Additional reason for this deviation might arise from the affinity of CO_2 that varies considerably depending on the type of polymer of interest.

The affinity of CO_2 for a polymer is associated with the interaction between CO_2 and the polymer. Fourier transform infrared (FTIR) spectroscopy has been used to investigate the interactions of CO_2 with polymers [14–17]. Although FTIR cannot be used to differentiate the states of CO_2 in the Henry mode from those in the Langmuir mode in glassy polymers [14], the technique provides evidence of specific interactions of polymers with CO_2 [17]. In Eckert's findings [17], polymers containing carbonyl groups act as an electron donor and exhibit a specific intermolecular interaction with CO_2 acting as an electron acceptor rather than as an electron donor. Johnston and coworkers [18] have also suggested that the interaction of CO_2 with polymers possessing acrylate groups (containing carbonyl groups) may be of a Lewis acid–base nature. Specific interactions were proposed to exist between CO_2 and the dipoles of C–F bonds [19] or fluorine [20] to explain the increased solubility of CO_2 in fluorine containing polymers. Weak electrostatic interactions [17,21] were proposed to exist between CO_2 and the π-system (phenyl ring) in PS. PS does not posses carbonyl groups and thus does not show strong Lewis acid–base interaction with CO_2. Polyethylene (PE) does not posses carbonyl groups as in poly(vinyl acetate) and π-system as in PS and thus does not show Lewis acid–base and electrostatic interactions, respectively. Therefore, the model to be used to describe the dissolution behavior for CO_2 in a polymer might considerably vary with the nature of the polymer.

For many polymers, the CO_2 sorption isotherms reported were measured in pressure range between 0 and up to 50 atm; the Langmuir capacity contribution was clearly observed at pressures less than about 5 atm depending on temperatures [2,3]. The Langmuir-type sorption is small as compared with the dissolution in the bulk polymer for high pressures [22]. The objective of this study is to measure CO_2 sorption isotherms over a wide pressure range 10–340 atm at 32 °C and sorption isobars for up to 340 atm over 25–52 °C for rubbery EVA. Factors affecting these isotherms and isobars are investigated. These factors involving the content of carbonyl groups from poly(vinyl acetate) (PVAc) segments and the degree of crystallinity of the crystalline phase from polyethylene segments are emphasized.

2. Experimental

2.1. Materials

Four types of EVA including EVA16, EVA18, EVA25, and EVA28 were used as received in a form of cylindrical pellets with a diameter ~4 mm and an axial length ~2.2 mm. EVA16 was supplied by USI Far East Corporation (Taipei, Taiwan) having a trade name UE630, a melt index 1.5 g/10 min, and a density 0.937 g/cm^3. EVA18 was supplied by DuPont Corporation having a trade name EVA460, a melt index 2.5 g/10 min, and a density 0.941 g/cm^3. EVA25 was supplied by USI Far East Corporation (Taipei, Taiwan) having a trade name UE659, a melt index 2.0 g/10 min, and a density 0.947 g/cm^3. EVA28 was supplied by Exxon Corporation having a trade name UL00328, a melt index 3.0 g/10 min, and a density 0.955 g/cm^3.

2.2. ^{1}H NMR analyses

The VA (vinyl acetate) contents in EVA samples were characterized by means of ^{1}H NMR (Bruker AMX 400, 400 MHz, $CDCl_3$) using TMS as a reference. The assignments of absorption peaks were as follows: 0.92 δ (methyl protons of polyethylene), 1.306 δ (methylene protons of polyethylene), 1.511 δ (methylene protons of poly(vinyl acetate)), 1.9 δ (methyl protons of poly(vinyl acetate)), and 4.917 δ (methine protons of poly(vinyl acetate)). The VA contents in the four EVA samples can be calculated from the ^{1}H NMR spectra (not shown in this paper) and are tabulated in Table 1.

2.3. DSC analyses

A differential scanning calorimeter (DSC2010, TA Instruments, New Castle, DE) was used for the thermal analysis for EVA samples prior to sorption experiments. The temperature reading and energy involved in DSC thermograms were calibrated with indium (mp 156.6 °C, $\Delta H_f = 6.8$ cal/g) and tin (mp 231.88 °C, $\Delta H_f = 14.45$ cal/g). To control the thermal history, all samples were first heated in DSC cell under nitrogen atmosphere at a rate of 10 °C/min to 200 °C and held for 3 min to eliminate the

Table 1
The VA contents of the four EVA samples characterized by ^{1}H NMR

Sample code	Weight fraction	Mole fraction
EVA 16	18.24	6.77
EVA 18	18.77	7.00
EVA 25	25.57	10.06
EVA 28	27.11	10.80

residual crystallites. The samples were then cooled at 10 °C/min to −70 °C, followed by heating at the same rate to 200 °C to obtain melting temperatures (T_m) and heats of fusion (ΔH_m). The percent crystallinity for the samples was determined by the ratio $\Delta H_m/\Delta H_{m100}$, where ΔH_m was the heats of fusion in joules per gram polyethylene segments in the EVA samples and ΔH_{m100} was the heat of fusion in joule per gram pure polyethylene with 100% crystallinity. The ΔH_{m100} is 281 J/g [23]. Poly(vinyl acetate) segments in the EVA copolymer was assumed to be non-crystalline in the calculation of the percent crystallinity of the sample.

2.4. Sorption measurements

All four EVA samples used in this study were cylindrical pellets with a volume of ~28 mm^3 for each pellet. The weight of a sample for the sorption measurement was ~3.1 g. The sorption measurements were performed in a supercritical extractor supplied by ISCO (Lincoln, Nebraska) with a model SFX 2–10 which was equipped with a syringe pump with a model 260D. The samples for the sorption measurements were put in a 10-cm^3 cell located inside the extractor pressurized by the equipped syringe-type pump. The extractor was controllable in pressure over the range 0–10,000 psi (680 atm) and in temperature over the range 20–100 °C. The pressurizing time for reaching any preset pressure below 680 atm was 30 s. The extractor was controlled at a preset temperature prior to the pressurizing. The exposure (soaking) time for the sample in CO_2 was 1 h which was experimentally confirmed to be long enough for the cylindrical pellet samples to reach equilibrium sorption concentration as shown in Figs. 1 and 2. After the exposure, the cell was depressurized to ambient pressure in 10 s and the sample inside the cell was then taken outside for weight measurement in another 10 s. The data of weight change was determined to be highly reproducible. The weight changes were measured outside the cell, not as measured in situ inside the cell, because the measurements were good enough to provide the equilibrium dissolution isotherms and isobars for the purpose of this study. After the measurements in weight changes, the samples were heated at 110 °C and vacuumed for 30 min to evacuate all dissolved CO_2 inside the sample. Such heating treatments demonstrated that the samples after sorption experiments showed a negligible EVA dissolution in CO_2.

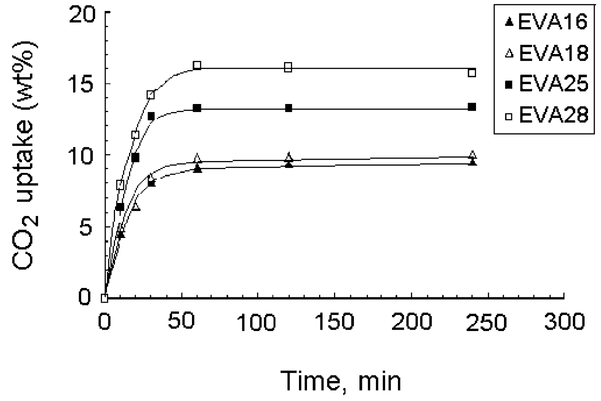

Fig. 1. The weight percent CO_2 uptakes for four EVA samples as a function of exposure time at 27 °C and 68 atm.

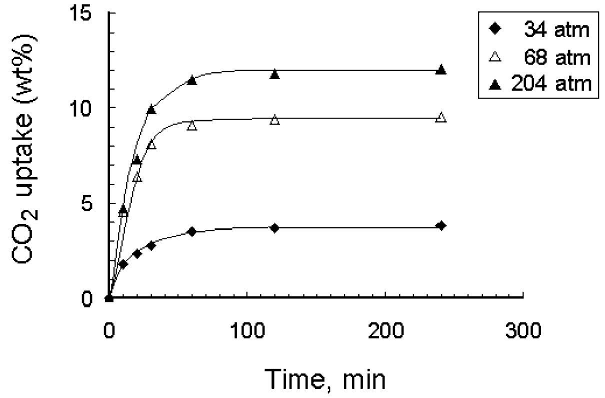

Fig. 2. The weight percent CO_2 uptakes for EVA16 as a function of exposure time at 32 °C and three pressures.

3. Results and discussion

As described in Section 2, all four EVA samples used in this study were not very thin film samples but were cylindrical pellets with a volume of ~28 mm^3 for each pellet. The purpose of this study is to investigate the equilibrium sorption isotherms and isobars through which the dissolution behavior of CO_2 in EVA is correlated with the CO_2 conditions. The equilibrium sorption, or more appropriately equilibrium solubility, refers to the saturated dissolution of CO_2 in EVA. For pellet samples in this study, it takes time to reach equilibrium sorption and to release the dissolved CO_2 in EVA. Provided that the depressurizing and the weighing for the sample after sorption experiment are complete in a very short time (totally 20 s in this study), it is not unreasonable to assume that the weight change obtained from the weighing outside the cell after the sorption experiment represents the total weight change due to the sorption process. Although the data of weight change obtained is not from the in situ weighing during the sorption process in this study, the data was confirmed to be highly reproducible and is good enough to provide the equilibrium dissolution isotherms and isobars for the purpose of this study.

Fig. 1 shows the weight percent CO_2 uptake (i.e. parts of CO_2 absorbed by 100 parts of EVA) for four EVA samples studied as a function of exposure time to CO_2 at 27 °C and 68 atm. The curves in Fig. 1 level off after 60 min of exposure, suggesting that the equilibrium solubility is reached at 60 min of exposure. In the initial 60 min exposure, the uptake rate is the highest for EVA28, followed by EVA25 and then by EVA18 and by EVA16. After 60 min of exposure, the leveled off percent uptakes show in a similar order as that for the uptake rates; i.e. EVA28 > EVA25 > EVA18 > EVA16. As tabulated in Table 1, the VA content of EVA sample is 10.80, 10.06, 7.00, and 6.77 mol% for EVA28, EVA25, EVA18, and EVA16, respectively. These VA contents suggest that both the uptake rate and the equilibrium solubility obtained are dictated by the carbonyl groups contents in the samples. Apparently, the higher carbonyl groups content leads to a higher CO_2 uptake rate and equilibrium solubility in the EVA sample.

Fig. 2 shows the percent CO_2 uptake for EVA16 as a function of exposure time to CO_2 at 27 °C for three different pressures. The curves in Fig. 2 again level off at 60 min of exposure for all three pressures studied, indicating that the equilibrium solubility is reached at 60 min of exposure independent of pressures. Both the uptake rate and the equilibrium solubility are dependent on pressures, with the 204 atm giving the highest uptake rate and the highest equilibrium solubility, followed by the 68 atm and then by the 34 atm. Since the density of CO_2 is a function of pressure, with the 204 atm having the highest and the 34 atm the least, the density (other than the pressure) could be the major factor to govern the sorption process. Based on the observation from Figs. 1 and 2, 60 min of exposure time is thus used to perform all sorption experiments to obtain equilibrium sorption isotherms and isobars.

Before the plots of equilibrium sorption isotherms and isobars are shown and discussed, the density of CO_2 being a function of pressure [24] needs to be taken into consideration. Fig. 3 shows the density of CO_2 as a function of pressure for some temperatures. As can be seen in Fig. 3, the density increases with increasing pressure in a manner that the density increasing is the most significant around P_c (72.8 atm), followed by that for pressures below about 50 atm and then by that for pressures above P_c. This most significant variation in density around P_c occurs at a higher pressure for a higher temperature. The CO_2 density at above P_c is mostly higher than 0.7 g/cm^3 for the four temperatures, indicative of liquid-like property for CO_2 at high pressures.

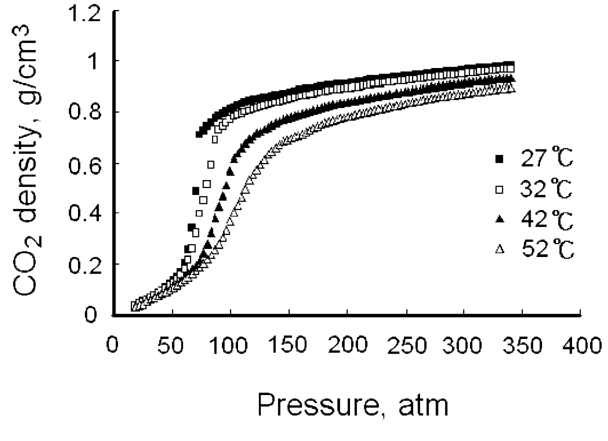

Fig. 3. The density of CO_2 as a function of pressure for 27, 32, 42, and 52 °C.

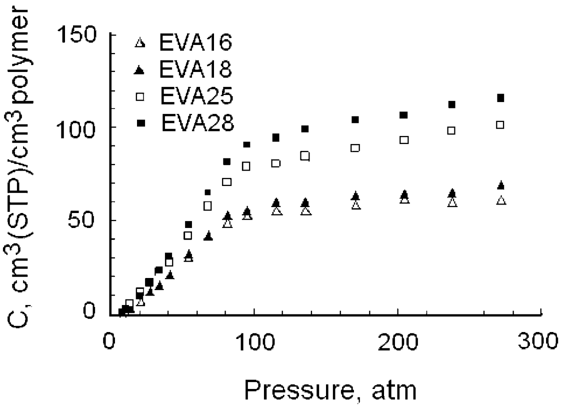

Fig. 4. The CO_2 sorption isotherms at 32 °C for four EVA samples as a function of CO_2 pressure.

Fig. 4 shows the equilibrium sorption concentration of CO_2 in EVA as a function of pressure at 32 °C for all four EVA samples. The sorption isotherm of each sample as a function of pressure in Fig. 4 can be roughly divided into two regions with P_c roughly at the border of the two regions. For below P_c, the curvature of the sorption isotherms is slightly concave upward whereas for above P_c the sorption isotherms are linearly functions of pressure. For sorption isotherms below P_c, the CO_2 dissolution behavior is similar to that reported by Kamiya and coworkers [12]. However, the EVA sample used in the previous study [12] containing 15 wt% of VA is different from the samples used in this study containing at least 18 wt% of VA. Also the temperature in the previous study is different from that in this study. Thus the dissolved CO_2 concentrations in the previous study are not compared with those in this study. When the dissolved CO_2 concentration is plotted as a function of CO_2 density as shown in Fig. 5, the sorption isotherms can be divided into three regions. According to Fig. 3, the region of density below ~0.2 g/cm^3 in Fig. 5 corresponds to the

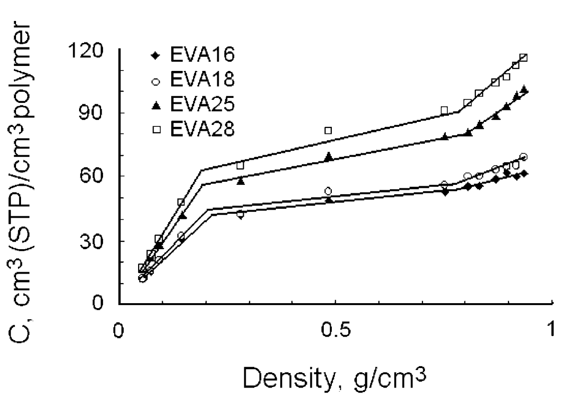

Fig. 5. The CO_2 sorption isotherms at 32 °C for four EVA samples as a function of CO_2 density.

gas CO_2 whereas the region of density above ~0.7 g/cm^3 corresponds to the supercritical CO_2. The density between ~0.2 and ~0.7 g/cm^3 corresponds to the transition region from gas to supercritical fluid. As can be seen in Fig. 5, the considerable increase in density in the transition region around P_c did not contribute a significant increase of the dissolved CO_2 concentration. This is probably due to a significant change in CO_2 properties (such as viscosity and diffusivity) over the transition region, resulting in a lessened density effect on the CO_2 dissolution in EVA. In addition, from Fig. 4, the dissolved CO_2 concentration for a given pressure is in the order of EVA28 > EVA25 > EVA18 > EVA16. This once again implies that the dissolution is driven by the carbonyl groups.

Thus far the content of carbonyl groups has been demonstrated as a major factor to affect the sorption isotherms (Figs. 1, 4, and 5). To investigate if other factors also affect the sorption isotherms, the normalized sorption concentrations in cm^3 (STP) CO_2 per mole VA unit are used to plot as a function of pressure as shown in Fig. 6. As can be seen in Fig. 6, the normalized sorption concentrations are almost the same for below P_c for all four EVA samples, suggesting that the content of carbonyl groups is the determining factor to the sorption process at below P_c. For above P_c, the normalized sorption concentrations at a pressure are different among samples in the order of EVA28 > EVA25 > EVA18 > EVA16. This result suggests that other factors come to play in the sorption process.

From DSC measurements for EVA samples, the endotherms of second heating scans, arising from the melting of the polyethylene segments in EVA, were used to determine the heats of fusion (ΔH_m), the melting temperatures (T_m), and the degrees of crystallinity ($X\%$) for samples as tabulated in Table 2. The T_m and $X\%$ in Table 2 both decrease with increasing VA content in EVA sample, an indication that the acetate groups can impede the crystallization. Based on the degree of crystallinity data in Table 2, the non-overlapping observation in the normalized sorption concentrations for a given pressure in Fig. 6 for above P_c may be attributed to the different sorption ability for crystalline and amorphous phase. Apparently, the crystalline phase has lower sorption ability than the amorphous phase because the normalized sorption concentrations increase with decreasing degrees of crystallinity. Thus, the crystallinity is a factor affecting the normalized sorption concentration above P_c, although it is an insignificant factor below P_c due to too strong effect of the carbonyl groups on the sorption process.

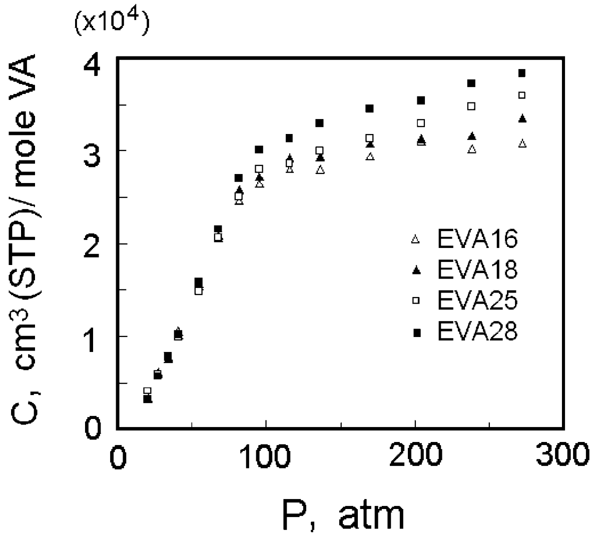

Fig. 6. The normalized CO_2 sorption concentration isotherms at 32 °C for four EVA samples as a function of CO_2 pressure.

Table 2
Melting temperatures (T_m), heats of fusion (ΔH_m), and degrees of crystallinity ($X\%$) for four EVA samples

Sample code	T_m (°C)	ΔH_m[a] (J/g)	$X\%$[b]
EVA 16	87.9	62.3	27.1
EVA 18	85.3	55.6	24.4
EVA 25	76.3	35.1	16.8
EVA 28	72.9	29.1	14.2

[a] The heat of fusion in joule per gram of sample. The value is divided by the weight fraction of polyethylene segment in EVA to obtain the heat of fusion in joule per gram polyethylene; e.g. for EVA16, 62.3 J/g EVA16 is divided by 0.8176 (from Table 1) to obtain 76.20 J/g polyethylene.

[b] $X\%$, the degree of crystallinity, is calculated by dividing the heat of fusion in joule per gram polyethylene in EVA by 281 J/g, the heat of fusion for 100% crystallinity of pure polyethylene.

Fig. 7 is the logarithmic plots for those normalized plots in Fig. 6. Fig. 7 is better than Fig. 4 to demonstrate two different sorption behaviors for a given EVA sample over a wide pressure range. The change in the sorption behavior for each EVA sample is found to occur at P_c. In other words, the sorption behavior for each EVA sample is different for below and above P_c. Based on the plots in Fig. 7, the two sorption behaviors for each EVA sample can be described by two power laws written as in Eqs. (2) and (3) other than by the dual mode model or other models:

$$C = k_a P^{n_a} \tag{2}$$

$$C = k_b P^{n_b} \tag{3}$$

where C is the equilibrium sorption concentration in a unit of cm^3 (STP) CO_2 per mole VA unit, P is pressure in atm, k_a, k_b, n_a, and n_b are constants. Eq. (2) is for describing the sorption behavior for above P_c whereas Eq. (3) is for below P_c. Apparently, both Eqs. (2) and (3) do not include contribution from either the Langmuir-type sorption or the Henry's law dissolution or the Flory–Huggins dissolution. In other words, neither can the Langmuir-type sorption mode nor the Henry's law dissolution mode nor the Flory–Huggins dissolution mode satisfactorily describe the observation on the CO_2 sorption behavior in Fig. 6. According to adsorption theory, the Langmuir adsorption model turns into a power law adsorption model, or Freundlich

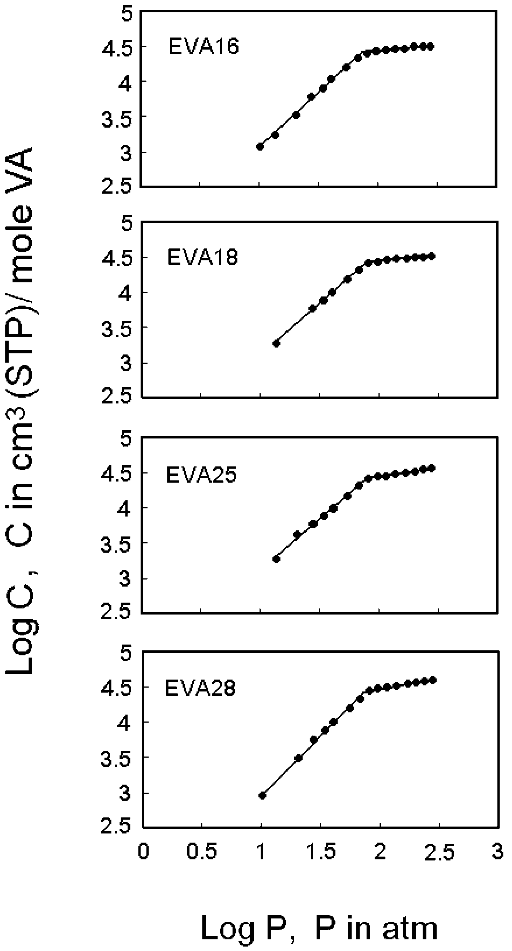

Fig. 7. The logarithmic normalized CO_2 sorption concentration isotherms at 32 °C as a function of the logarithmic CO_2 pressure for four EVA samples.

adsorption model (named after the originator), as the adsorption surfaces are no longer homogeneous and the variation in the parameter b in the Langmuir model is attributed entirely to a variation in the heat of adsorption [25]. Thus, it is not unreasonable to propose the power law to describe the dissolution behavior of CO_2 in EVA because the location inside EVA at which the CO_2 molecule is dissolved can be considered a heterogeneous environment.

The k_a, k_b, n_a, and n_b values calculated from Fig. 7 are tabulated in Table 3. For a polymer, k_a and k_b give a measure of sorption capacity whereas n_a and n_b give a measure of sorption intensity according to the Freundlich adsorption theory. As can be seen in Table 3 for below P_c, the sorption capacity constants and sorption intensity constants are not absolutely irrelevant to the composition of the polymer, suggesting that the carbonyl group content is not the only factor to affect the sorption behavior. This is understandable from Fig. 6 where the normalized isotherms at near P_c are not fully overlapped, indicating that other factors than just the carbonyl group content has come to affect the sorption process. These other factors might include the crystallinity and/or the plasticization effect at near P_c. These factors appear to be insignificant at pressures far below P_c because fully overlapped isotherms were observed. For above P_c, the effect of crystallinity becomes significant to affect the sorption isotherms leading to an increasing sorption intensity (n_a) but a decreasing sorption capacity (k_a) as the degree of crystallinity decreases. This indicates that the sorption capacity is closely associated with the degree of crystallinity whereas the sorption intensity is closely associated with the interaction of CO_2 and polymer. The sorption capacity of the polymers for above P_c is about 2–3 times higher than that for below P_c, suggesting that the density of CO_2 is a major factor affecting the solubility of CO_2 in EVA. The sorption intensity of the polymers for above P_c is about seven times lower than that for below P_c, suggesting that other CO_2 properties, perhaps viscosity and diffusivity, are determining factors affecting the solubility of CO_2 in EVA.

Table 3
The k_a, n_a, k_b, and n_b values calculated from Fig. 7 for Eqs. (2) and (3)

Sample code	Below P_c		Above P_c	
	k_b	n_b	k_a	n_a
EVA 16	1.52	1.54	4.07	0.17
EVA 18	1.58	1.50	4.05	0.19
EVA 25	1.70	1.43	3.89	0.27
EVA 28	1.28	1.69	3.87	0.29

The sorption isotherms that can be described by power laws in this work over a wide pressure range 10–340 atm are different from those described by the dual mode model in Koros and Paul's study [3] over the pressure range 0– ~ 30 atm and by the Flory–Huggins theory in Kamiya and coworkers' study over 0–50 atm [12]. A difference is also found as compared with those in Wissinger and Paulaitis's work [26] over 0–100 atm. In this previous work [26], the CO_2 sorption isotherms for polycarbonate (PC) having a T_g 147 °C, poly(methyl methacrylate) (PMMA) having a T_g 105 °C, and polystyrene (PS) having a T_g 100 C at elevated pressures up to 100 atm over a temperature range 33–65 °C were investigated. The sorption behavior for these polymers was found to depend on the occurrence of a glass transition induced by the CO_2 sorption. Two distinct types of sorption isotherms were measured. Without the occurrence of a glass transition for the polymer (e.g. PC at 35 °C, PMMA at 32.7 °C) during sorption experiments, the sorption isotherms reached limiting values at elevated pressures whereas the isotherms continued to increase with pressure resulting in an upward concave curvature for the polymer (e.g. PMMA at 42.0 and 58.8 °C, PS at 35.0, 50.0, and 65 °C) involving a glass transition. Accordingly, EVA should exhibit a sorption isotherm continuing to increase with increasing pressure at elevated pressures because EVA, having a T_g well below the experimental temperature in this work, does not involve a glass transition during the sorption experiments. As shown in Fig. 4, however, EVA exhibits a very slow increase in sorption concentration at

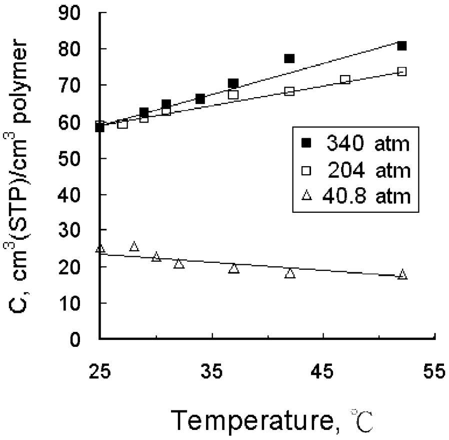

Fig. 8. The CO_2 sorption isobars for EVA16 as a function of temperature.

above P_c. The sorption behavior that has been observed in this work is, apparently, not consistent with the results from the previous work [26]. The disparities between this work and previous studies [3,12,26] are due to differences in experimental techniques. In this work, pellets samples were used and the sorption experiments were done up to 340 atm. In the previous studies, thin films were used and the experiments were done up to only ~30 [3] or 50 [12] or 100 atm [26]. CO_2 at these low pressures giving low CO_2 densities was too low in solvent power to give high CO_2 sorption concentrations in the polymer. In addition, the sorption capacity of the polymer is limited by the thin thickness of the sample. This restricted the previous studies [3,12,26] on the sorption behavior to the low-pressure region.

Fig. 8 presents sorption isobars for EVA16 for three pressures over 25–52 °C. With increasing temperature, the sorption decreases for the 40.8 atm whereas the sorption increases for the 204 and 340 atm. Fig. 9 presents the plots of sorption isobars for three pressures as a function of CO_2 density. As can be seen in Fig. 9, for the 40.8 atm CO_2 is in gaseous state and the density of CO_2 is not drastically varied with temperature. The considerable decrease in the sorption for the 40.8 atm with insignificant decrease (caused by increasing temperature) in CO_2 density suggests that the viscosity of gaseous CO_2 might govern the sorption isobar of the 40.8 atm because the viscosity of gaseous CO_2 increases with increasing temperature [27]. The effect of density on the sorption isobars for the 204 and 340 atm is more pronounced than the 40.8 atm. The direction of the effect from the 204 and 340 atm is, however, opposite from the 40.8 atm. For the 204 and 340 atm, CO_2 is in either liquid or supercritical state depending on temperature. The viscosity of CO_2 decreases whereas the diffusivity of CO_2 increases with increasing temperature leading to increasing sorption concentration at a given pressure.

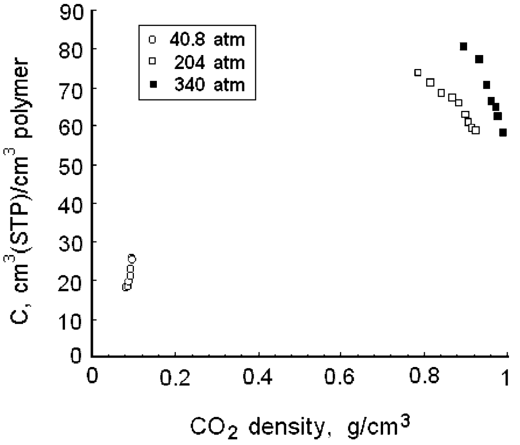

Fig. 9. The CO_2 sorption isobars for EVA16 as a function of CO_2 density.

4. Conclusions

The equilibrium CO_2 sorption isotherms and isobars for rubbery EVA containing various amounts of vinyl acetate (VA) over a wide pressure range 10–340 atm and 25–52 °C were investigated. It was found that the normalized CO_2 sorption concentration (C, in cm^3 (STP) CO_2/mole VA) isotherms of these polymers as a function of pressure (P) consisted of two distinct regions turning at P_c and could be fairly described by two respective power laws $C = kP^n$ other than by the dual mode model or the simplified Flory–Huggins model as reported previously. For the isobars, with increasing temperature, the sorption decreased for the 40.8 atm (CO_2 in gaseous state) whereas the sorption increased for the 204 and 340 atm (CO_2 in either liquid or supercritical state). The viscosity of gaseous CO_2 increased whereas that of liquid or supercritical CO_2 decreased with increasing temperature leading to a decreasing sorption for the 40.8 atm and an increasing sorption for the 204 and 340 atm.

Acknowledgements

We thank National Science Council of Republic of China for financial support for this work.

References

[1] Barrer RM, Barrie JA, Slater J. J Polym Sci 1958;27:177.
[2] Koros WJ, Paul DR, Rocha AA. J Polym Sci, Polym Phys Ed 1976;14:687.
[3] Koros WJ, Paul DR. J Polym Sci, Polym Phys Ed 1978;16:1947.
[4] Vieth WR, Howell JM, Hsieh JH. J Membr Sci 1976;1:177.
[5] Michaels AS, Vieth WR, Barrie JA. J Appl Phys 1963;34:1.
[6] Frisch HL. Polym Engng Sci 1980;20:2.
[7] Berens AR, Huvard GS. In: Johnston KP, Penninger JML, editors. Supercritical fluid science and technology, ACS Symposium Series 406. Washington, DC: American Chemical Society, 1989. Chapter 14.
[8] Kamiya Y, Mizoguchi K, Naito Y, Hirose T. J Polym Sci, Part B: Polym Phys 1986;24:535.

[9] Kamiya Y, Hirose T, Mizoguchi K, Naito Y. J Polym Sci, Part B: Polym Phys 1986;24:1525.
[10] Fleming GK, Koros WJ. Macromolecules 1986;19:2285.
[11] Stern SA, DeMeringo AH. J Polym Sci, Polym Phys Ed 1978;16:735.
[12] Kamiya Y, Naito Y, Bourbon D. J Polym Sci, Part B: Polym Phys 1994;32:281.
[13] Suwandi MS, Stern SA. J Polym Sci, Part B: Polym Phys 1973;11:663.
[14] Higuchi A, Nakagawa T. J Polym Sci, Part B: Polym Phys 1994;32:149.
[15] Briscoe BJ, Kelly CT. Polymer 1995;36:3099.
[16] Fried JR, Li W. J Appl Polym Sci 1990;41:1123.
[17] Kazarian SG, Vincent MF, Bright FV, Liotta CL, Eckert CA. J Am Chem Soc 1996;118:1729.
[18] Mawson S, Johnston KP, Combes JR, DeSimone JM. Macromolecules 1995;28:3182.
[19] Tuminello WH, Dee GT, McHugh MA. Macromolecules 1995;28:1506.
[20] Shah VM, Hardy BJ, Stern SA. J Polym Sci, Part B: Polym Phys 1993;31:313.
[21] Nandel FS, Jain DVS. Indian J Chem 1984;23A:543.
[22] Chang SH, Park SC, Shim JJ. J Supercrit Fluids 1998;13:113.
[23] Brandrup J, Immergut EH. Polymer handbook. 3rd ed. New York: Wiley, 1989.
[24] Kroschwitz JI, Howe-Grant M. Kirk-Othmer Encyclopedia of Chemical Technology. 4th ed, vol. 23. New York: Wiley, 1997. p. 452.
[25] Adamson AW. Physical chemistry of surfaces. 5th ed. New York: Wiley, 1990.
[26] Wissinger RG, Paulaitis ME. J Polm. Sci, Part B: Polym Phys 1987;25:2497.
[27] Welty JR, Wicks CE, Wilson RE. Fundamentals of momentum, heat, and mass transfer. 3rd ed. New York: Wiley, 1984.